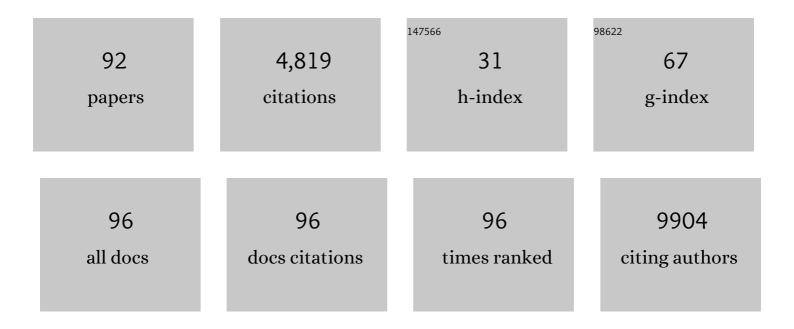
BalÃ;zs GulyÃ;s

List of Publications by Year in descending order

Source: https://exaly.com/author-pdf/2057506/publications.pdf Version: 2024-02-01



ΒΛΙ Δισς ΟιμνΔις

#	Article	IF	CITATIONS
1	Positron emission tomographic imaging in drug discovery. Drug Discovery Today, 2022, 27, 280-291.	3.2	21
2	Mollification of Doxorubicin (DOX)-Mediated Cardiotoxicity Using Conjugated Chitosan Nanoparticles with Supplementation of Propionic Acid. Nanomaterials, 2022, 12, 502.	1.9	7
3	The Multifarious Applications of Copper Nanoclusters in Biosensing and Bioimaging and Their Translational Role in Early Disease Detection. Nanomaterials, 2022, 12, 301.	1.9	16
4	Gadolinium and Polythiophene Functionalized Polyurea Polymer Dots as Fluoro-Magnetic Nanoprobes. Nanomaterials, 2022, 12, 642.	1.9	1
5	Differential effects of white matter hyperintensities and regional amyloid deposition on regional cortical thickness. Neurobiology of Aging, 2022, 115, 12-19.	1.5	5
6	The Exoproteome of Staphylococcus pasteuri Isolated from Cervical Mucus during the Estrus Phase in Water Buffalo (Bubalus bubalis). Biomolecules, 2022, 12, 450.	1.8	1
7	Shallow 3D CNN for Detecting Acute Brain Hemorrhage From Medical Imaging Sensors. IEEE Sensors Journal, 2021, 21, 14290-14299.	2.4	65
8	Doxorubicin-Conjugated Platinum Theranostic Nanoparticles Induce Apoptosis <i>via</i> Inhibition of a Cell Survival (PI3K/AKT) Signaling Pathway in Human Breast Cancer Cells. ACS Applied Nano Materials, 2021, 4, 198-210.	2.4	14
9	An In Vivo Study of a Rat Fluid-Percussion-Induced Traumatic Brain Injury Model with [11C]PBR28 and [18F]flumazenil PET Imaging. International Journal of Molecular Sciences, 2021, 22, 951.	1.8	7
10	Fluorescence ResonanceÂEnergy TransferÂ(FRET)-Based ThT Free Sensing of Beta-Amyloid Fibrillation by Carbon Dot-Ag Composites. Plasmonics, 2021, 16, 863-872.	1.8	3
11	Auditory steady-state responses during and after a stimulus: Cortical sources, and the influence of attention and musicality. Neurolmage, 2021, 233, 117962.	2.1	7
12	Parkinson's Disease: A Nanotheranostic Approach Targeting Alpha-Synuclein Aggregation. Frontiers in Cell and Developmental Biology, 2021, 9, 707441.	1.8	10
13	Positive and Negative Impacts of COVID-19 in Digital Transformation. Sustainability, 2021, 13, 9470.	1.6	18
14	Alzheimer's Disease: A Molecular View of β-Amyloid Induced Morbific Events. Biomedicines, 2021, 9, 1126.	1.4	22
15	Gold Nano-Urchins Enhanced Surface Plasmon Resonance (SPR) BIOSENSORS for the Detection of Estrogen Receptor Alpha (ERα). IEEE Journal of Selected Topics in Quantum Electronics, 2021, 27, 1-6.	1.9	5
16	An Overview on Cognitive Function Enhancement through Physical Exercises. Brain Sciences, 2021, 11, 1289.	1.1	15
17	Amyloid Beta42 (Aβ42) Peptide Functionalized Iron Oxide Nanoparticles for Specific Targeting of SH-SY5Y Neuroblastoma Cells. Journal of Nanoscience and Nanotechnology, 2021, 21, 5044-5050.	0.9	0
18	Anticancer Potential of L-Histidine-Capped Silver Nanoparticles against Human Cervical Cancer Cells (SiHA). Nanomaterials, 2021, 11, 3154.	1.9	3

BALÃiZS GULYÃiS

#	Article	IF	CITATIONS
19	Codon usage of human hepatitis C virus clearance genes in relation to its expression. Journal of Cellular Biochemistry, 2020, 121, 534-544.	1.2	1
20	Blood brain barrier: A tissue engineered microfluidic chip. Journal of Neuroscience Methods, 2020, 331, 108525.	1.3	15
21	Targeted pancreatic beta cell imaging for early diagnosis. European Journal of Cell Biology, 2020, 99, 151110.	1.6	5
22	Altered striatal dopamine levels in Parkinson's disease VPS35 D620N mutant transgenic aged mice. Molecular Brain, 2020, 13, 164.	1.3	10
23	3D Deep Learning on Medical Images: A Review. Sensors, 2020, 20, 5097.	2.1	268
24	Attentional modulation of the auditory steady-state response across the cortex. NeuroImage, 2020, 217, 116930.	2.1	13
25	Mushroom-Derived Carbon Dots for Toxic Metal Ion Detection and as Antibacterial and Anticancer Agents. ACS Applied Nano Materials, 2020, 3, 5910-5919.	2.4	146
26	Au nano-urchins enabled localized surface plasmon resonance sensing of beta amyloid fibrillation. Nanoscale Advances, 2020, 2, 2693-2698.	2.2	17
27	Gadolinium-based bimodal probes to enhance T1-Weighted magnetic resonance/optical imaging. Acta Biomaterialia, 2020, 110, 15-36.	4.1	28
28	Nanotheranostic agents for neurodegenerative diseases. Emerging Topics in Life Sciences, 2020, 4, 645-675.	1.1	10
29	Dealing with PET radiometabolites. EJNMMI Research, 2020, 10, 109.	1.1	9
30	Misfolded Protein Linked Strategies Toward Biomarker Development for Neurodegenerative Diseases. Molecular Neurobiology, 2019, 56, 2559-2578.	1.9	2
31	Peripheral Biomarkers for Early Detection of Alzheimer's and Parkinson's Diseases. Molecular Neurobiology, 2019, 56, 2256-2277.	1.9	43
32	The gut microbiota influences skeletal muscle mass and function in mice. Science Translational Medicine, 2019, 11, .	5.8	271
33	In vitro phosphodiesterase 10A (PDE10A) binding in whole hemisphere human brain using the PET radioligand [18F]MNI-659. Brain Research, 2019, 1711, 140-145.	1.1	6
34	Bifunctional Fluorescent/Raman Nanoprobe for the Early Detection of Amyloid. Scientific Reports, 2019, 9, 8497.	1.6	34
35	Muscle extract of Arothron immaculatus regulates the blood glucose level and the antioxidant system in high-fat diet and streptozotocin induced diabetic rats. Bioorganic Chemistry, 2019, 90, 103072.	2.0	7
36	PET-MR and SPECT-MR multimodality probes: Development and challenges. Theranostics, 2018, 8, 6210-6232.	4.6	59

BALÃiZS GULYÃiS

#	Article	IF	CITATIONS
37	Theranostic applications of nanoparticles in neurodegenerative disorders. International Journal of Nanomedicine, 2018, Volume 13, 5561-5576.	3.3	102
38	PET/MRI: a frontier in era of complementary hybrid imaging. European Journal of Hybrid Imaging, 2018, 2, 12.	0.6	38
39	Thallium Labeled Citrate-Coated Prussian Blue Nanoparticles as Potential Imaging Agent. Contrast Media and Molecular Imaging, 2018, 2018, 1-10.	0.4	14
40	Buffalo nasal odorant-binding protein (bunOBP) and its structural evaluation with putative pheromones. Scientific Reports, 2018, 8, 9323.	1.6	14
41	Lineage-specific exosomes could override extracellular matrix mediated human mesenchymal stem cell differentiation. Biomaterials, 2018, 182, 312-322.	5.7	66
42	The small molecule AUTEN-99 (autophagy enhancer-99) prevents the progression of neurodegenerative symptoms. Scientific Reports, 2017, 7, 42014.	1.6	37
43	27-Hydroxycholesterol impairs neuronal glucose uptake through an IRAP/GLUT4 system dysregulation. Journal of Experimental Medicine, 2017, 214, 699-717.	4.2	64
44	Engineering Concepts in Stem Cell Research. Biotechnology Journal, 2017, 12, 1700066.	1.8	9
45	The Advents of Hybrid Imaging Modalities: A New Era in Neuroimaging Applications. Advanced Biology, 2017, 1, e1700019.	3.0	10
46	Current Perspective of Stem Cell Therapy in Neurodegenerative and Metabolic Diseases. Molecular Neurobiology, 2017, 54, 7276-7296.	1.9	30
47	An automated method measures variability in P-glycoprotein and ABCG2 densities across brain regions and brain matter. Journal of Cerebral Blood Flow and Metabolism, 2017, 37, 2062-2075.	2.4	20
48	Peptides functionalized carbon dots for in vitro fluorescent imaging of amyloid fibrils. , 2017, , .		0
49	An Overview of Multimodal Neuroimaging Using Nanoprobes. International Journal of Molecular Sciences, 2017, 18, 311.	1.8	9
50	Theranostic Probes for Targeting Tumor Microenvironment: An Overview. International Journal of Molecular Sciences, 2017, 18, 1036.	1.8	43
51	Structural elucidation of estrus urinary lipocalin protein (EULP) and evaluating binding affinity with pheromones using molecular docking and fluorescence study. Scientific Reports, 2016, 6, 35900.	1.6	9
52	AUTEN-67 (Autophagy Enhancer-67) Hampers the Progression of Neurodegenerative Symptoms in a Drosophila model of Huntington's Disease. Journal of Huntington's Disease, 2016, 5, 133-147.	0.9	39
53	Nanoparticulate Contrast Agents for Multimodality Molecular Imaging. Journal of Biomedical Nanotechnology, 2016, 12, 1553-1584.	0.5	30
54	Multi-functional nano silver: A novel disruptive and theranostic agent for pathogenic organisms in real-time. Scientific Reports, 2016, 6, 34058.	1.6	21

BALÃiZS GULYÃiS

#	Article	IF	CITATIONS
55	Proteomic analysis of human saliva: An approach to find the marker protein for ovulation. Reproductive Biology, 2016, 16, 287-294.	0.9	11
56	Guidelines to PET measurements of the target occupancy in the brain for drug development. European Journal of Nuclear Medicine and Molecular Imaging, 2016, 43, 2255-2262.	3.3	28
57	Nanoparticles in practice for molecular-imaging applications: An overview. Acta Biomaterialia, 2016, 41, 1-16.	4.1	175
58	Brain PET measurement of PDE10A occupancy by TAKâ€063, a new PDE10A inhibitor, using [¹¹ C]Tâ€773 in nonhuman primates. Synapse, 2016, 70, 253-263.	0.6	15
59	Acute neuroinflammation in a clinically relevant focal cortical ischemic stroke model in rat: longitudinal positron emission tomography and immunofluorescent tracking. Brain Structure and Function, 2016, 221, 1279-1290.	1.2	49
60	A PET study comparing receptor occupancy by five selective cannabinoid 1 receptor antagonists in non-human primates. Neuropharmacology, 2016, 101, 519-530.	2.0	12
61	AUTEN-67, an autophagy-enhancing drug candidate with potent antiaging and neuroprotective effects. Autophagy, 2016, 12, 273-286.	4.3	50
62	Evaluation of a novel <scp>PDE</scp> 10 <scp>A</scp> <scp>PET</scp> radioligand, [¹¹ <scp>C</scp>] <scp>T</scp> â€₹73, in nonhuman primates: Brain and whole body <scp>PET</scp> and brain autoradiography. Synapse, 2015, 69, 345-355.	0.6	18
63	Positron Emission Tomography studies with [11C]PBR28 in the Healthy Rodent Brain: Validating SUV as an Outcome Measure of Neuroinflammation. PLoS ONE, 2015, 10, e0125917.	1.1	11
64	InÂvivo occupancy of the 5-HT1A receptor by a novel pan 5-HT1(A/B/D) receptor antagonist, GSK588045, using positron emission tomography. Neuropharmacology, 2015, 92, 44-48.	2.0	4
65	Decrease of mGluR5 receptor density goes parallel with changes in enkephalin and substance P immunoreactivity in Huntington's disease: a preliminary investigation in the postmortem human brain. Brain Structure and Function, 2015, 220, 3043-3051.	1.2	14
66	Biocompatible branched copolymer nanoparticles prepared by RAFT polymerization as MRI/PET bimodal tracers. EJNMMI Physics, 2015, 2, A90.	1.3	0
67	Synthesis of antibacterial and magnetic nanocomposites by decorating graphene oxide surface with metal nanoparticles. RSC Advances, 2015, 5, 76442-76450.	1.7	41
68	The gut microbiota influences blood-brain barrier permeability in mice. Science Translational Medicine, 2014, 6, 263ra158.	5.8	1,589
69	Exploration of salivary proteins in buffalo: an approach to find marker proteins for estrus. FASEB Journal, 2014, 28, 4700-4709.	0.2	17
70	MicroRNAs -the Next Generation Therapeutic Targets in Human Diseases. Theranostics, 2013, 3, 930-942.	4.6	68
71	Performance Evaluation of the Small-Animal nanoScan PET/MRI System. Journal of Nuclear Medicine, 2013, 54, 1825-1832.	2.8	104
72	János Szentágothai. 31 October 1912 — 8 September 1994. Biographical Memoirs of Fellows of the Royal Society, 2013, 59, 383-406.	0.1	0

#	Article	IF	CITATIONS
73	Distribution and binding of 18F-labeled and 125I-labeled analogues of ACI-80, a prospective molecular imaging biomarker of disease: A whole hemisphere post mortem autoradiography study in human brains obtained from Alzheimer's disease patients. Neurochemistry International, 2012, 60, 153-162.	1.9	8
74	Evolution of microglial activation in ischaemic core and peri-infarct regions after stroke: A PET study with the TSPO molecular imaging biomarker [C]vinpocetine. Journal of the Neurological Sciences, 2012, 320, 110-117.	0.3	81
75	Visualising Neuroinflammation in Post-Stroke Patients: A Comparative PET Study with the TSPO Molecular Imaging Biomarkers [¹¹ C]PK11195 and [¹¹ C]vinpocetine. Current Radiopharmaceuticals, 2012, 5, 19-28.	0.3	41
76	Age and disease related changes in the translocator protein (TSPO) system in the human brain: Positron emission tomography measurements with [11C]vinpocetine. NeuroImage, 2011, 56, 1111-1121.	2.1	80
77	Activated MAO-B in the brain of Alzheimer patients, demonstrated by [11C]-l-deprenyl using whole hemisphere autoradiography. Neurochemistry International, 2011, 58, 60-68.	1.9	171
78	The norepinephrine transporter (NET) radioligand (S,S)-[18F]FMeNER-D2 shows significant decreases in NET density in the human brain in Alzheimer's disease: A post-mortem autoradiographic study. Neurochemistry International, 2010, 56, 789-798.	1.9	62
79	A comparative autoradiography study in post mortem whole hemisphere human brain slices taken from Alzheimer patients and age-matched controls using two radiolabelled DAA1106 analogues with high affinity to the peripheral benzodiazepine receptor (PBR) system. Neurochemistry International, 2009, 54, 28-36.	1.9	66
80	FDG, MET or CHO? The quest for the optimal PET tracer for glioma imaging continues. Nature Clinical Practice Neurology, 2008, 4, 470-471.	2.7	11
81	Summary: The Budapest meeting 2005 intensified networking on ethics of science. Science and Engineering Ethics, 2006, 12, 415-420.	1.7	1
82	Synthesis and PET evaluation of (R)-[S-methyl-11C]thionisoxetine, a candidate radioligand for imaging brain norepinephrine transporters. Journal of Labelled Compounds and Radiopharmaceuticals, 2006, 49, 1007-1019.	0.5	14
83	[11C]Vinpocetine: a prospective peripheral benzodiazepine receptor ligand for primate PET studies. Journal of the Neurological Sciences, 2005, 229-230, 219-223.	0.3	44
84	Effect of amphetamine on dopamine D2 receptor binding in the primate brain with the agonist ligand [11C]MNPA. Journal of Cerebral Blood Flow and Metabolism, 2005, 25, S646-S646.	2.4	0
85	The putative pheromone androstadienone activates cortical fields in the human brain related to social cognition. Neurochemistry International, 2004, 44, 595-600.	1.9	44
86	Monkeys ??? a great asset to reveal human cognitive functions. NeuroReport, 2002, 13, 2167-2168.	0.6	1
87	Cerebral uptake of [ethyl-11C]vinpocetine and 1-[11C]ethanol in cynomolgous monkeys: a comparative preclinical PET study. Nuclear Medicine and Biology, 2002, 29, 753-759.	0.3	13
88	Radiochemical labelling of the dopamine D3 receptor ligand RGH-1756. Journal of Labelled Compounds and Radiopharmaceuticals, 2000, 43, 1069-1074.	0.5	10
89	Neuronal correlates of real and illusory contour perception: functional anatomy with PET. European Journal of Neuroscience, 1999, 11, 4024-4036.	1.2	117
90	Cerebral Effects of a Single Dose of Intravenous Vinpocetine in Chronic Stroke Patients: A PET Study. Journal of Neuroimaging, 1998, 8, 197-204.	1.0	38

#	Article	IF	CITATIONS
91	Cortical fields participating in spatial frequency and orientation discrimination: Functinal anatomy by positron emission tomography. Human Brain Mapping, 1995, 3, 133-152.	1.9	22
92	Processing and Analysis of Form, Colour and Binocular Disparity in the Human Brain: Functional Anatomy by Positron Emission Tomography. European Journal of Neuroscience, 1994, 6, 1811-1828.	1.2	66